

# Determination of the orbital parameters of binary pulsars

Bhaswati Bhattacharyya,<sup>1</sup> Rajaram Nityananda<sup>1</sup>

<sup>1</sup>National Centre for Radio Astrophysics, TIFR, Pune University Campus, Post Bag 3, Pune 411 007, India

Accepted. Received

## ABSTRACT

We present a simple method for determination of the orbital parameters of binary pulsars, using data on the pulsar period at multiple observing epochs. This method uses the circular nature of the velocity space orbit of Keplerian motion and produces preliminary values based on two one dimensional searches. Preliminary orbital parameter values are then refined using a computationally efficient linear least square fit. This method works for random and sparse sampling of the binary orbit. We demonstrate the technique on (a) the highly eccentric binary pulsar PSR J0514–4002 (the first known pulsar in the globular cluster NGC 1851) and (b) 47 Tuc T, a binary pulsar with a nearly circular orbit.

**Key words:** Stars: neutron – stars: pulsars: general – stars: pulsar: individual:

## 1 INTRODUCTION

Knowledge of the orbital parameters of binary pulsars is necessary for coherent timing and for investigation of different properties of the pulsar and the companion star. Determination of the orbital parameters is important for newly discovered pulsars, to plan follow up observations at different epochs.

With the movement of the binary pulsar in its orbit around the center of mass, the projected velocity of the pulsar in the line of sight direction ( $v_l$ ) changes and as a consequence the observed pulsar period ( $P_{obs}$ ) changes. The modulation in  $v_l$  (i.e. in  $P_{obs}$ ) is governed by the orbital parameters of the binary system. So it is possible to get information about the orbit by studying the evolution of  $P_{obs}$ . Five orbital parameters, namely, the binary orbital period ( $P_b$ ), orbital eccentricity ( $e$ ), projection of the semi major axis on the line of sight ( $a_1 \sin i$ ,  $i$  being the angle between the orbit and the sky plane), longitude of periastron ( $\omega$ ) and the epoch of periastron passage ( $T_o$ ) can be determined from radial velocity/observed pulsar period data (in the Newtonian, i.e non-relativistic regime). These orbital parameters of binary pulsar systems can be determined by fitting a Keplerian model to the pulsar period versus epoch of observation data. The usual methods require simultaneous fit to many parameters and need an initial guess. Such methods need dense sampling of period measurements at different epochs during the pulsar orbital period. Overcoming some of these factors, Freire et al. (2001b) proposed a new method for determination of the orbital parameters of binary pulsars. They utilised information on periods and period derivatives at multiple observing epochs of the kind used in surveys, and extracted orbital parameter values. They successfully determined the orbital parameters of binary pulsars with nearly circular orbits.

This work presents an alternative approach to orbital parameter determination using the observing epoch versus pulsar period

data, without requiring information about pulsar period derivatives. We demonstrate the method by estimating the orbital parameters of the binary pulsar PSR J0514–4002A, the first known pulsar in the globular cluster NGC 1851 (Freire et al. 2004), and PSR J0024–7204, a binary pulsar in globular cluster 47 Tucanae, referred to as 47 Tuc T hereafter (Camilo et al. 2000). In Sect.2 we describe the method for preliminary determination of the orbital parameters. Sect.3 presents a method for refinement of the determined orbital parameters. In Sect.4 we compare the orbital parameters determined in this work with those available in the literature and discuss the advantages of our method.

## 2 PRELIMINARY DETERMINATION OF ORBITAL PARAMETERS

### 2.1 Binary orbital period ( $P_b$ )

The observed pulsar period ( $P_{obs}$ ) versus epoch of observation data set is folded with wide range of trial orbital periods ( $P_b$ ). Corresponding to each trial value of  $P_b$ , we get,  $P_{obs}$  versus orbital phase ( $\phi = 2\pi t/P_b$ ,  $t$  being the time measured from the periastron). For every set of folded data we calculate a parameter – roughness ( $R$ ) – which we define as the summation of squared differences of  $P_{obs}$  between the adjacent pairs of  $\phi$ . Therefore,

$$R = \sum_{i=1}^n (P_{obs}(i) - P_{obs}(i+1))^2 \quad (1)$$

where  $n$  represents the total number of data points. These points are sorted in order of orbital phase, which will be different for different choices of trial  $P_b$ . For the optimal choice of the trial folding period  $P_b$ , the plot of  $P_{obs}$  versus  $\phi$  is expected to be the smoothest and hence the corresponding roughness parameter ( $R$ ) will be min-

arXiv:0803.1907v2 [astro-ph] 3 Apr 2008

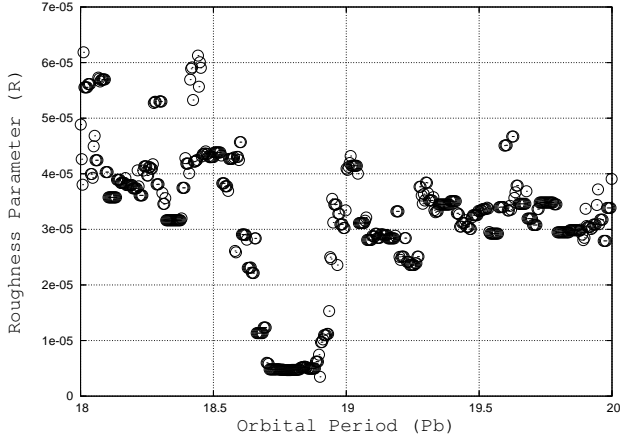


**Figure 1.** Roughness parameter ( $R$ ) plotted against orbital period ( $P_b$ ) for PSR J0514–4002A (a zoomed region near minimum  $R$ )

imum. In the search of  $P_b$  the increment ( $\Delta P_b$ ) must be chosen to cause small orbital phase shift (i.e.  $\Delta\omega_b T \ll 1$ ) over the full data length  $T$  (i.e.  $(2\pi/P_b^2)\Delta P_b T \ll 1$ ).

As a crosscheck, we apply this method on a simulated Keplerian orbit. First, we simulate sparsely and randomly sampled epoch of observation versus radial velocity data points with a set of arbitrarily chosen  $P_b$ ,  $e$ ,  $\omega$  and  $T_o$  values (refer to Eqn. 6 of Sect. 2.2 for details). Using this kind of randomly generated radial velocity data, spanning over widely separated epochs, as input we apply the smoothness criterion described in Eqn. 1 and the true binary orbital period is recovered. There are few local minimas where  $R$  is lower than the adjacent values but there is no comparable minimum as to the strongest minimum corresponding to true  $P_b$ . The method worked for Keplerian orbits generated with various sets of  $P_b$ ,  $e$ ,  $\omega$  and  $T_o$  values, and we could reproduce the true periodicity. Hence, to obtain a unique solution for  $P_b$ , one need to search for  $P_b$  within a wide range which includes the actual  $P_b$  with small enough step size determined by the criterion  $(2\pi/P_b^2)\Delta P_b T \ll 1$ .

For preliminary determination of  $P_b$  of PSR J0514–40, we used  $P_{obs}$  versus epoch of observation data from the GMRT observations. We used 31 such data points, collected over six months, which are similar to the data used for Freire et al. (2004). For the known binary pulsars in globular clusters the orbital periods lie in the range  $P_b \sim$  few hours to 256 days (refer to Table 1.1 of Freire et al. (2000)). Initially we try  $P_b$  starting from few hours and up to 300 days with step size satisfying the criterion  $(2\pi/P_b^2)\Delta P_b T \ll 1$ , and determine  $R$  using Eqn.1. Then we narrowed down our search of the  $P_b$  around the lowest  $R$ . Though there are few local minima where  $R$  is lower than the adjacent values, we observe the strongest and rather flat minimum for a range of nearby values of  $P_b$  s around 18.79 days, no comparable minimum is observed in the range from few hours to 300 days. Fig. 1 presents the plot of the trial  $P_b$  against the corresponding  $R$ , zoomed into a region where  $R$  is minimum. For  $P_b=18.791$  days  $R$  is minimum. We fold the data with  $P_b=18.791$  days to generate  $P_{obs}$  versus  $\phi$  data set (see Fig.2).

For the determination of orbital period of 47 Tuc T we utilised the 9 data points (provided in Freire et al. (2001b)) of  $P_{obs}$  versus epoch of observation. We determine  $P_b=1.1$  days which is close to the value estimated by Freire et al. (2001b).

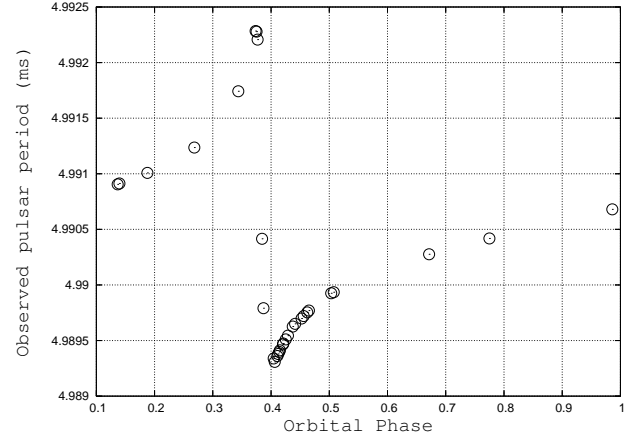


**Figure 2.** Orbital phase ( $\phi$ ) versus observed pulsar period ( $P_{obs}$ ) of PSR J0514–4002A after folding the data with  $P_b=18.791$  days

## 2.2 Other orbital parameters from the hodograph

The left panel of Fig. 3 shows the orbit of a binary pulsar around the center of mass of the system, projected in a plane containing the direction of Earth and the line of nodes (line of intersection of orbital plane and the sky plane). 'A' denotes the periastron position and  $\theta$  is the angle of the pulsar to the periastron, also known as 'true anomaly'. 'B' and 'C' are two other points in the binary orbit. A rather geometric picture of the Kepler's laws using the idea of velocity space is due to Hamilton (1847). It is not often used and hence described briefly below. According to Newton's laws for the path of the vector  $(\vec{r}_{pulsar}(t) - \vec{r}_{companion}(t))$  (i.e. for the relative orbit of the pulsar with respect to the companion star), the relative velocity,

$$\Delta \mathbf{v} = - \left( \frac{GM}{r^2} \right) \Delta t \hat{\mathbf{r}} \quad (2)$$

where  $G$  is the Gravitational constant and  $M$  is the total mass of the pulsar and the companion star.

From the conservation of angular momentum,

$$\Delta \theta = \frac{h}{r^2} \Delta t \quad (3)$$

where  $h$  is angular momentum per unit mass.

Dividing the absolute value of Eqn. 2 by Eqn. 3 we get,

$$\frac{|\Delta \mathbf{v}|}{\Delta \theta} = \left( \frac{GM}{h} \right) = constant \quad (4)$$

The path followed by the velocity vector of a particle is called the hodograph.  $\Delta \mathbf{v}$  is the arc length and  $\Delta \theta$  is the angle traversed by the pulsar in velocity space. The ratio  $(|\Delta \mathbf{v}|/\Delta \theta)$  is the radius of curvature of the hodograph. Since the radius of curvature is constant, the hodograph is a circle for Keplerian motion. The right panel of Fig.3 shows the corresponding hodograph of the elliptical binary orbit that is shown in the left panel. The center of the circle is offset from the origin by  $(eGM/h)$  and the radius of the circle is  $(GM/h)$ .

For a particular eccentricity ( $e$ ) and longitude of periastron ( $\omega$ ), the  $x$  and  $y$  component of velocity are given by,

$$v_x = - \frac{GM}{h} \sin \theta; \quad v_y = \frac{GM}{h} (\cos \theta + e) \quad (5)$$

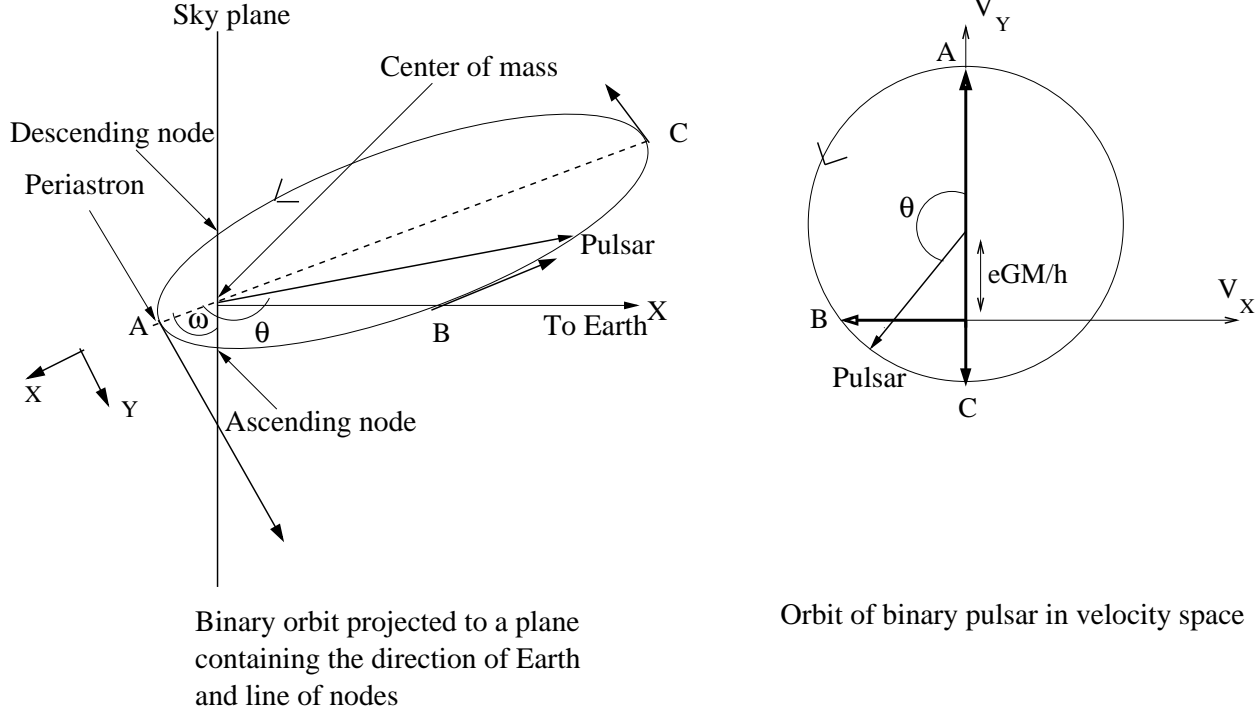


Figure 3. Binary orbit

Hence, the relative radial velocity along the projection of the line of sight into the orbital plane is given by,

$$\begin{aligned}
 v_r &= (v_x \cos(\pi/2 - \omega) + v_y \sin(\pi/2 - \omega)) \\
 &= \left(\frac{GM}{h}\right) (\sin \theta \sin \omega + (\cos \theta + e) \cos \omega) \\
 &= \left(\frac{GM}{h}\right) v_{r_s}
 \end{aligned} \tag{6}$$

For  $\omega = 90^\circ$  the observed velocity will be antisymmetric (odd) as a function of  $\theta$  or time measured from periastron. Similarly, for  $\omega = 0^\circ$  the observed velocity will be symmetric (even). For other intermediate values of  $\omega$  the observed velocity will be a combination of antisymmetric and symmetric parts in the ratio of  $\sin \omega / \cos \omega$ . Plot of the antisymmetric versus the symmetric part will be an ellipse and the parameters of the ellipse will provide preliminary values of the orbital parameters.

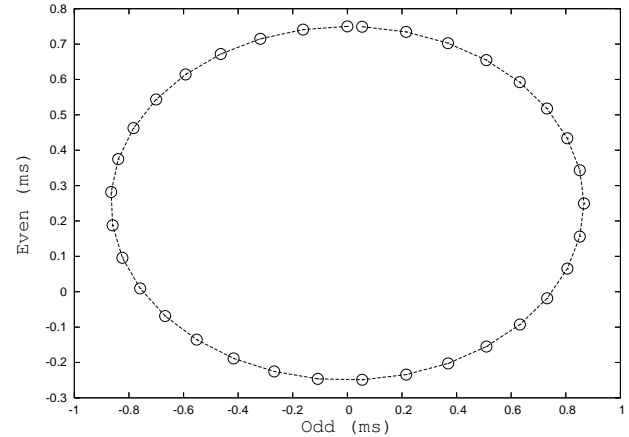
As a crosscheck, we apply this method on simulated Keplerian orbits. We simulate  $v_{r_s}$  for trial value of  $e$ ,  $\omega$  and  $T_o$ . Corresponding to each  $v_{r_s}$  value at a particular orbital phase ( $\phi$ ), we determine the  $v_{r_s}$  at conjugate phase ( $2\pi - \phi$ ), using Lagrange's interpolation method with three points. The even and odd parts are defined as follows,

$$v_{r_s}^{even} = (v_{r_s}(\phi) + v_{r_s}(2\pi - \phi))/2 \tag{7}$$

$$v_{r_s}^{odd} = (v_{r_s}(\phi) - v_{r_s}(2\pi - \phi))/2 \tag{8}$$

Plot of  $v_{r_s}^{odd}$  versus  $v_{r_s}^{even}$  should be an ellipse, for correct choice of  $T_o$  (Fig.4). The ratio of major and the minor axes of the ellipse gives,  $\tan \omega$ , and the shift of the origin of the ellipse gives  $e$ . Using the method illustrated in Appendix A, we fit an ellipse to the  $v_{r_s}^{odd}$  versus  $v_{r_s}^{even}$  data.  $\omega$  and  $e$  are recovered from the parameters of the best fit ellipse.

Since  $v_{r_s}$  and the observed pulsar period ( $P_{obs}$ ) will have similar modulations, we construct antisymmetric and symmetric parts


 Figure 4.  $v_{r_s}^{odd}$  versus  $v_{r_s}^{even}$  (generated for simulated Keplerian orbit with  $e = 0.5$ ,  $\omega = 60^\circ$ ) and the fitted ellipse for correct choice of  $T_o$ 

from the  $P_{obs}$ . Corresponding to each  $P_{obs}$  value at a particular orbital phase ( $\phi$ ), we determine the  $P_{obs}$  at conjugate phase ( $2\pi - \phi$ ) using Lagrange's interpolation method with three points. The even and the odd parts are defined as follows,

$$P_{obs}^{even} = (P_{obs}(\phi) + P_{obs}(2\pi - \phi))/2 \tag{9}$$

$$P_{obs}^{odd} = (P_{obs}(\phi) - P_{obs}(2\pi - \phi))/2 \tag{10}$$

The plot of  $P_{obs}^{odd}$  versus  $P_{obs}^{even}$  should be an ellipse for correct choice of the periastron passage ( $T_o$ ). We vary  $T_o$ , corresponding  $P_{obs}^{odd}$  versus  $P_{obs}^{even}$  are generated, and fit an ellipse to the  $P_{obs}^{odd}$  versus  $P_{obs}^{even}$  plot (Appendix A). The left panel of Fig. 5 is the plot of  $P_{obs}^{odd}$  versus  $P_{obs}^{even}$  for real data of 47 Tuc T with arbitrary choice of  $T_o$ . The right panel of Fig. 5 is the plot of  $P_{obs}^{odd}$  versus  $P_{obs}^{even}$

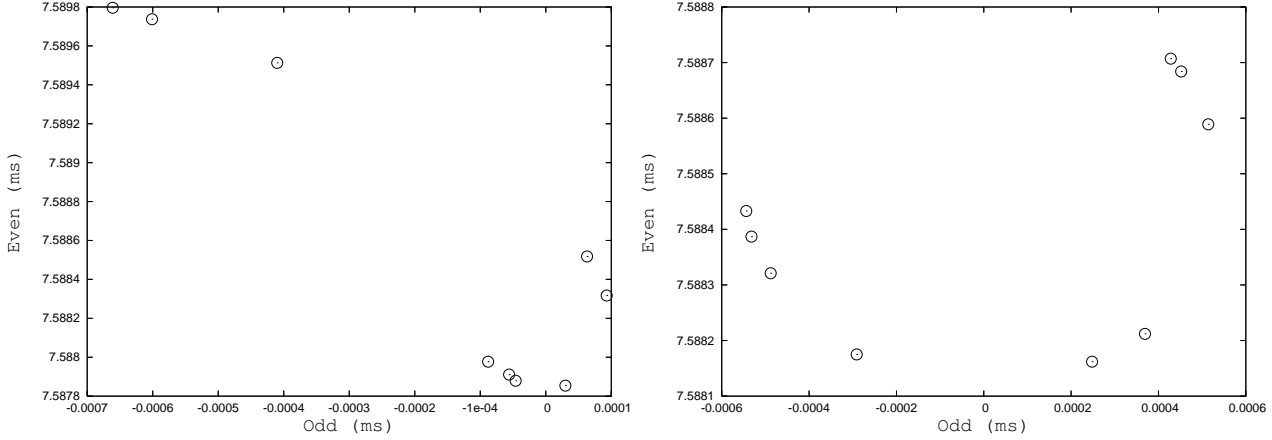


**Figure 5.**  $P_{obs}^{odd}$  versus  $P_{obs}^{even}$  for 47 Tuc T for arbitrary choice of  $T_o$  (left panel) and correct choice of  $T_o$  with minimum  $\chi^2$  (right panel)

for real data of 47 Tuc T with optimal choice of  $T_o$  ( $T_o$  for which  $\chi^2$  is minimum after ellipse fitting). Preliminary values of  $e$ ,  $\omega$  are obtained from the parameters of the best fit ellipse (Appendix A).

### 3 REFINEMENT OF THE DETERMINED ORBITAL PARAMETERS

In this section we take the preliminary determined orbital parameters as the initial guess in a linear least squares fit. This is now computationally efficient since only a small range of the parameters, near the first guess values, has to be searched.  $P_{obs}$  is determined by the relation,

$$P_{obs} = P_o \left(1 + \frac{v_l}{c}\right) \quad (11)$$

where  $P_o$  is the rest frame period of the binary pulsar,  $v_l$  is the projected velocity of the pulsar in the line of sight direction and  $c$  is the velocity of light. This relationship is valid provided  $v_l$  is small compared to  $c$ .

Following are the steps for determination of orbital parameters:

1. We simulate orbital phase ( $\phi$ ) versus scaled radial velocity ( $v_{r,s}$ ) with trial values  $P_b$ ,  $e$ ,  $\omega$ ,  $T_o$  (using Eqn. 6).
2. To compare the simulated data with the observations we need to find out the simulated  $v_{r,s}$  at those orbital phase points for which  $P_{obs}$  is available.  $v_{r,s}$  at observed orbital phases is obtained by using Lagrange's interpolation method with three points.
3. Next we fit a straight line to  $P_{obs}$  versus  $v_{r,s}$  and calculate  $\chi^2$ .

We repeat this procedure for all the trial combinations of orbital parameters. As shown in the Appendix B, for the right choice of the orbital parameters, the plot of  $P_{obs}$  versus  $v_{r,s}$  will be a straight line (see Eqn. B8). Hence, the set of orbital parameters,  $P_b$ ,  $e$ ,  $\omega$ ,  $T_o$ , for which the straight line fit is best, i.e.  $\chi^2$  value is minimum, will correspond to the optimal choice of orbital parameters.  $\chi^2$  is minimised so that the expected value for  $N$  independent data points is  $N$ . A change of 1 then corresponds to a 68% confidence limit (page 694, Press et al. (1992)). Given the above criterion for change in  $\chi^2$ , the optimal grid for any parameter (keeping all the other parameter fixed) would have about three points in an interval over which the minimum  $\chi^2$  ( $\chi^2_{min}$ ) increases by 1  $\sigma$  ( $\sigma \sim \chi^2_{min}/N$ ). This is the criterion that decide the step size

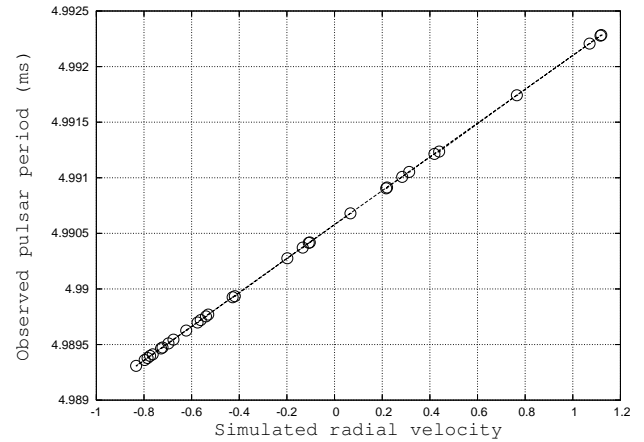


**Figure 6.** Simulated radial velocity ( $v_{r,s}$ ) interpolated at each observing epoch is plotted against observed pulsar period ( $P_{obs}$ ) for PSR J0514-4002

used for different trial combinations of the orbital parameters. The search for each orbital parameter was continued till the  $\chi^2$  becomes about 1000  $\sigma$  on each side of the minima, keeping all the other parameters fixed. It is possible to use this method to determine the orbital parameters, with out assuming the preliminary values. But in that case one has to search a wide range for each of the orbital parameters which would be computationally expensive. The intercept of the fitted straight line will give the value of  $P_o$ . Substituting the values of  $P_b$ ,  $e$ ,  $P_o$  and the slope of the fitted straight line  $S_{fit}$ , in Eqn. B10, we can determine the projected semi major axis in light seconds,  $a_1 \sin(i)/c$ .

#### Implementation of the method

**(1) J0514-4002 :** Fig.6 presents the plot of  $P_{obs}$  versus  $v_{r,s}$  (generated with the optimal choice of orbital parameters) and the corresponding straight line fit. The residual from the best fit straight line are small for all the measurements, indicating successful fitting and orbital parameter determination. Table. 1 lists the determined orbital parameter values of PSR J0514-4002. The step size used for the different sets of trial of orbital parameters,  $P_b$ ,  $e$ ,  $\omega$  and  $T_o$ , are also listed in Table. 1. The uncertainty on the values of each of the orbital parameters are calculated from the change of orbital parameter values required for 1 $\sigma$  change in the  $\chi^2$  value, keeping all

**Table 1.** Orbital parameters of PSR J0514–4002

Parameter	Freire et al. (2004) (Period analysis)	Freire et al. (2007) (Coherent timing analysis)	This work
Orbital period ( $P_b$ ) (days)	18.7850(8)	18.7851915(4)	18.7851(1) [0.00003] <sup>‡</sup>
Eccentricity ( $e$ )	0.889(2)	0.8879773(3)	0.8879(2) [0.000005] <sup>‡</sup>
Longitude of periastron ( $\omega$ ) ( $^\circ$ )	82(1)	82.266550(18)	82.20(6) [0.002] <sup>‡</sup>
Semi major axis of the orbit projected along LOS ( $a_1 \sin(i)/c$ ) (light-seconds)	36.4(2)	36.2965(9)	36.28(1)
Pulsar period ( $P_o$ ) (ms)	4.990576(5)	4.990575114114(3)	4.990575(4)
Epoch of periastron passage ( $T_o$ ) (MJD)	52984.46(2)	-	52984.5(1) [0.02] <sup>‡</sup>

† : The uncertainty quoted in the bracket is on the last significant digit of the concerned parameter.

‡ : The step size used for comparing the simulation with the observation (Sect. 3).

**Table 2.** Orbital parameters of 47 Tuc T

Parameter	Freire et al. (2001b) (Acceleration analysis)	Freire et al. (2001a) (Coherent timing analysis)	This work
Orbital period ( $P_b$ ) (days)	1.12(3)	1.126176785(5)	1.126175(2) [0.0000005] <sup>‡</sup>
Eccentricity ( $e$ )	-	0.00038(2)	0.0000(8) [0.0001] <sup>‡</sup>
Longitude of periastron ( $\omega$ ) ( $^\circ$ )	-	63(3)	63.0(1) [0.03] <sup>‡</sup>
Semi major axis of the orbit projected along LOS ( $a_1 \sin(i)/c$ ) (light-seconds)	1.33(4)	1.33850(1)	1.337(2)
Pulsar period ( $P_o$ ) (ms)	7.588476(4)	7.588479792132(5)	7.58848(2)
Epoch of periastron passage ( $T_o$ ) (MJD)	51000.3173(2)	51000.317049(2)	51000.317(2) [0.0001] <sup>‡</sup>

† : The uncertainty quoted in the bracket is on the last significant digit of the concerned parameter.

‡ : The step size used for comparing the simulation with the observation (Sect. 3).

the other parameters fixed. The uncertainty quoted in the bracket is on the last significant digit of the concerned parameter.

(2) **47 Tuc T** : Fig.7 plots the  $P_{obs}$  versus the optimal  $v_{rs}$ . It is evident that the observational data is well reproduced. Determined orbital parameter values and the associated errors are listed in Table. 2.

## 4 DISCUSSION

The orbital parameters determined in this paper and those determined by Freire et al. (2004) and Freire et al. (2007) for PSR J0514–4002 are listed in Table. 1. For PSR J0514–4002, we have used similar data to those used by Freire et al. (2004) (Sect. 2). The orbital parameters determined by us are close to their determination within the error quoted by them. But our results are more accurate

and are close to the values obtained by Freire et al. (2007) who have used a much longer data stretch from regular observations with the GBT for about two years. Table. 2 compare the orbital parameters determined by us with those obtained by, Freire et al. (2001b) and Freire et al. (2001a) for 47 Tuc T. Our result agree with Freire et al. (2001b), but are more accurate and closer to the values predicted by Freire et al. (2007), who used coherent timing analysis for orbital parameter determination. Note that the small eccentricity of 47 Tuc T could only be found from the coherent timing solution. Our method of orbital parameter determination has the following features :

(1) The procedure for determination of binary orbital parameters outlined in this paper utilises the measurements of  $P_{obs}$  at given observing epoch and does not require any information about the period derivatives in contrast to the method described by Freire et al.

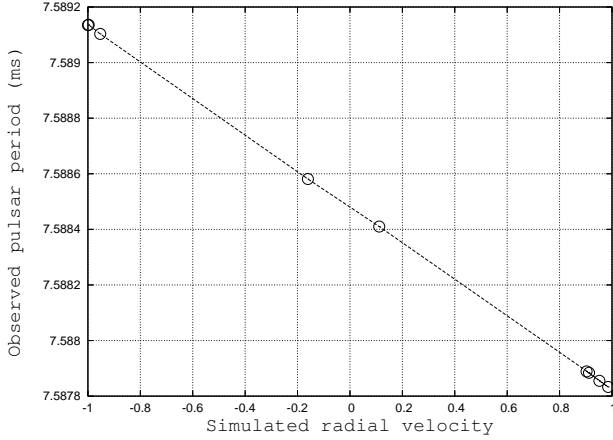


Figure 7. Same as Fig. 4 for 47 Tuc T

(2001b). It may at first sight be surprising that period derivatives do not help to constrain the final orbital solution. This can be understood by examining the accuracy of the measurement which is limited by the period variation over the length of a single observing session. Clearly, the period derivatives implied by the  $P_{obs}$  versus  $\phi$  curves already have smaller errors than this, since one is looking at period variations over the  $P_b$  time scale. However, period derivatives clearly plays a role in the work by Freire et al. (2001b) in determining orbital phases and  $P_b$ , which in our method comes from the roughness search.

(2) Unlike the method used by Freire et al. (2001b), which works for nearly circular binary orbits, this method works for binary orbit with any eccentricity. For example, our method worked well for the binary orbit with highest known eccentricity (PSR J0514–4002 with  $e \sim 0.888$ ), and also for an orbit with lower eccentricity (PSR 47 Tuc T with  $e \sim 0$ ).

(3) The accuracy of the determined orbital parameter values are subject to the sampling of the binary orbit. Our method works with random sampling of the orbit. A small number of data points are required for determination of orbital parameters in our method. In case of PSR J0514–4002, our method converged even for 5 random data points.

(4) The computation involves only one dimensional searches and linear least square fits<sup>1</sup>.

## 5 ACKNOWLEDGMENTS

We thank Yashwant Gupta for the data on PSR J0514–4002 used in this paper and for his comments. We thank Paulo C. Freire for a very useful discussion during his visit to NCRA. We are thankful to Subhashis Roy for critical reading of the draft and to Jayanta Roy for helping with coding. We are also thankful to an anonymous referee for his suggestions towards improvements of the paper.

<sup>1</sup> The code we have used consists of several stand alone programs in the 'octave' (matlab like) language. These programs have not been linked to make up a pipeline. Readers interested in the code may contact the authors.

## REFERENCES

- Camilo F., Lorimer D. R., Freire P. C., Lyne A. G. & Manchester R. N., 2000, *ApJ*, **535**, 975  
 Freire P. C., 2000, Ph.D. Thesis, Department of Physics and Astronomy, University of Manchester  
 Freire P. C., Camilo F., Lorimer D. R., Lyne A. G., Manchester R. N. & D'Amico N., 2001a, *MNRAS*, **326**, 901  
 Freire P. C., Kramer M., & Lyne A. G., 2001b, *MNRAS*, **322**, 885  
 Freire P. C., Gupta Y., Ransom S. M., & Ishwara-Chandra, C. H., 2004, *ApJ*, **606**, L53  
 Freire P. C., Ransom S. M., & Gupta Y., 2007, *ApJ*, **662**, 1177  
 Hamilton W. R., 1847, *Proceedings of the Royal Irish Academy*, **3**, 344, also available at this URL : <http://www.maths.soton.ac.uk/EMIS/classics/Hamilton/>  
 Press W. H., Teukolsky S. A., Vetterling W. T., Flannery B. P., 1992, *Numerical Recipes: The art of Scientific Computing*, 2nd edn. Cambridge Univ. Press, Cambridge

This paper has been typeset from a  $\text{\TeX}$   $\text{\LaTeX}$  file prepared by the author.

## APPENDIX A: FITTING AN ELLIPSE TO THE EVEN VERSUS ODD DATA

For fitting an ellipse to a set of points ( $P_{obs}^{even}$  versus  $P_{obs}^{odd}$ ) we use the information that the origin of the ellipse will be at  $(0, (eGM/h) \cos \omega)$ , and the major and minor axis of the ellipse will be  $(GM/h) \sin \omega$  and  $(GM/h) \cos \omega$ . Using this information we get an expression which is linear in parameters and hence is easy to fit. The ellipse will be of the form,

$$\frac{X^2}{\left(\frac{GM}{h} \sin \omega\right)^2} + \frac{(Y - e\frac{GM}{h} \cos \omega)^2}{\left(\frac{GM}{h} \cos \omega\right)^2} = 1 \quad (\text{A1})$$

Replacing  $(GM/h) \sin \omega = a$ ,  $(GM/h) \cos \omega = b$ ,  $(eGM/h) \cos \omega = d$  we have,

$$\frac{X^2}{a^2} + \frac{(Y - d)^2}{b^2} = 1 \quad (\text{A2})$$

Which can easily be simplified to the form,

$$AX^2 + BY^2 + CY = 1 \quad (\text{A3})$$

Where  $A = (1/a^2)/(1 - b^2/d^2)$ ,  $B = (1/b^2)/(1 - b^2/d^2)$ ,  $C = -(2d/b^2)/(1 - b^2/d^2)$ . We use the singular value decomposition method, as described by Press et al. (1992) (Freire et al. (2001b) used this method) to determine  $A$ ,  $B$  and  $C$ .<sup>2</sup>  $\chi^2$  in this case is defined as,

$$\chi^2 = \sum_{i=1}^N ((A (P_{obs}^{odd})_i^2 + B (P_{obs}^{even})_i^2 + C (P_{obs}^{even})_i) - 1)^2 \quad (\text{A4})$$

Here,  $\chi^2$  means deviations of the points normal to the ellipse. Criterion of minimising the  $\chi^2$  value gave us satisfactory results. From parameters of the fitted ellipse ( $A$ ,  $B$  and  $C$ ) we determine  $a$ ,  $b$  and  $c$  and obtain  $e$ ,  $\omega$  values as,  $e = d/b$  and  $\omega = \tan^{-1}(a/b)$ .

<sup>2</sup> While doing the ellipse fitting for the real data we used  $P_{obs}^{odd}$  versus mean subtracted  $P_{obs}^{even}$  data to avoid numerical problems.

**APPENDIX B: ILLUSTRATION OF THE STRAIGHT LINE NATURE OF OBSERVED PULSAR PERIOD VERSUS SIMULATED RADIAL VELOCITY PLOT**

Here we explain the straight line nature of  $P_{obs}$  versus  $v_{r,s}$  plot and interpret the slope and intercept in terms of the orbital parameters. We consider the binary orbit of the pulsar, where  $m_p$  and  $v_p$  are the mass and velocity of the pulsar and  $m_c$  and  $v_c$  are the same for the companion.  $a$  is the semi major axis of the pulsar orbit relative to the companion and  $a_1$  is the semi major axis of the pulsar relative to the center of mass. Using the standard relation between mass and specific angular momentum in a Kepler orbit we make the following illustrations for the relative orbit of the pulsar with respect to the companion.

$$\frac{GM}{h} = \frac{G(m_p + m_c)}{\sqrt{a(1 - e^2)G(m_p + m_c)}} \quad (\text{B1})$$

$$v_r = (v_p - v_c) = \frac{m_p + m_c}{m_c} v_p \quad (\text{B2})$$

$$a = a_1 \frac{m_p + m_c}{m_c} \quad (\text{B3})$$

Substituting  $GM/h$  (from Eqn. B1) in Eqn. 6,

$$v_r = \sqrt{\frac{G(m_p + m_c)}{a(1 - e^2)}} \times v_{r,s} \quad (\text{B4})$$

Therefore velocity of the pulsar  $v_p$  can be obtained from Eqn. B2 as,

$$v_p = \frac{m_c}{m_p + m_c} \sqrt{\frac{G(m_p + m_c)}{a(1 - e^2)}} \times v_{r,s} \quad (\text{B5})$$

Projected velocity of the pulsar in the line of sight direction ( $v_l$ ) is given by,

$$v_l = v_p \times \sin i = \frac{m_c}{m_p + m_c} \sqrt{\frac{G(m_p + m_c)}{a(1 - e^2)}} \times v_{r,s} \times \sin i \quad (\text{B6})$$

Therefore,  $v_l$  versus  $v_{r,s}$  is a straight line with slope ( $S$ ),

$$S = \frac{m_c}{m_p + m_c} \sqrt{\frac{Gm_c}{a_1(1 - e^2)}} \sin i \quad (\text{B7})$$

So  $P_{obs}$  versus  $v_{r,s}$  will also be a straight line with slope ( $S_{fit}$ ),

$$S_{fit} = \frac{P_o}{c} \times S \quad (\text{B8})$$

But  $P_b$  and  $a_1$  are related by,

$$P_b^2 = \frac{4\pi^2 a_1^3}{G} \left( \frac{(m_p + m_c)^2}{m_c^3} \right) \quad (\text{B9})$$

Therefore, from Eqn. B8 and Eqn. B9,

$$(a_1 \sin i)^2 = \frac{P_b^2 S_{fit}^2 (1 - e^2) c^2}{4\pi^2 P_o^2} \quad (\text{B10})$$